**Title: Sediment delivery and lake dynamics in a Mediterranean mountain watershed: Human-climate interactions during the last millennium (El Tobar Lake record, Iberian Range, Spain)**

**Name(s) and address(es) of the author(s) and email, telephone numbers:**
**1. (Corresponding author)** Fernando Barreiro-Lostres, Dpt. of Geo-environmental Processes and Global Change, Pyrenean Institute of Ecology – CSIC, Spain. Email: ferbalos@ipe.csic.es Tel.: +34 976.369.393 (ext. 880050).

**2.** Erik Brown, Large Lakes Observatory and Department of Geological Sciences, University of Minnesota Duluth, Duluth, MN 55812, USA. Email: etbrown@d.umn.edu Tel.: +1 218-726-8891.

**3.** Ana Moreno, Dpt. of Geo-environmental Processes and Global Change, Pyrenean Institute of Ecology – CSIC, Spain Email: amoreno@ipe.csic.es Tel.: +34 976369393 (ext. 880049).

**4.** Mario Morellón, Instituto de Geociencias (CSIC, UCM), Calle José Antonio Nováis, 2, 3ª planta, 3b, Facultad de Ciencias Geológicas, Univ. Complutense, 28040 Madrid, Spain. Email: mario.morellon@igeo.ucm-csic.es Tel.: +34 913944813

**5.** Mark Abbott, University of Pittsburgh, Geology and Planetary Science. 4107 O'Hara Street, Room 200, SRCC Building Pittsburgh, PA 15260-3332. USA. Email: mabbott1@pitt.edu Tel.: +1 412-624-1408.

**6.** Aubrey Hillman, University of Pittsburgh, Geology and Planetary Science. 4107 O'Hara St., SRCC 316, Pittsburgh, PA 15260-3332. USA. Email: alh118@pitt.edu Tel.: +1 412-624-8731.

**7.** Santiago Giralt, Institute of Earth Sciences Jaume Almera (ICTJA-CSIC), C/ Lluis Solé Sabaris s/n, Barcelona, E-08028 Spain. Email: sgiralt@ictja.csic.es Tel.: +34 934.095.410 (ext. 242).

**8.** Blas Valero-Garcés, Dpt. of Geo-environmental Processes and Global Change, Pyrenean Institute of Ecology – CSIC, Spain. Email: blas@ipe.csic.es Tel.: +34 976.369.393 (ext. 880050).

## Abstract

Land degradation and soil erosion are key environmental problems in Mediterranean mountains characterized by a long history of human occupation and a strong variability of hydrological regimes. To assess recent trends and evaluate climatic and anthropogenic impacts in these highly human modified watersheds we apply an historical approach combining lake sediment core multi-proxy analyses and reconstructions of past land uses to El Tobar Lake watershed, located in the Iberian Range (Central Spain). Four main periods of increased sediment delivery have been identified in the 8 m long sediment sequence by their depositional and geochemical signatures. They took place around 16$^{th}$, late 18$^{th}$, mid 19$^{th}$ and early 20$^{th}$ centuries as a result of large land uses changes such as forest clearing, farming and grazing during periods of increasing population. In this highly human-modified watershed, positive synergies between human impact and humid periods led to increased sediment delivery periods. During the last millennium, the lake depositional and geochemical cycles recovered quickly after each sediment delivery event, showing strong resilience of the lacustrine system to watershed disturbance. Recent changes are characterized by large hydrological affections since 1967 with the construction of a canal from a nearby reservoir and a decreased in anthropic pressure in the watershed as rural areas were abandoned. The increased fresh water influx to the lake has caused large biological changes, leading to stronger meromictic conditions and higher organic matter accumulation while terrigenous inputs have decreased. Degradation processes in Iberian Range watersheds are strongly controlled by anthropic activities

(land use changes, soil erosion) but modulated by climate-related hydrological changes (water availability, flood and runoff frequency).

**Keywords (6)**

Late Quaternary, Iberian Peninsula, karstic lake, geochemistry, sediment delivery, land use changes, palaeohydrology, resilience

## 1. Introduction

Water and soil are two of the most important natural resources for historical and modern societies and the availability of both creates a unique link between people and their environment (Stern, 2006). This especially applies to the Mediterranean region characterized by a fragile hydrologic and environmental equilibrium with frequent droughts and severe flooding (Benito et al., 2008; Lionello et al., 2012). This is the case of the Iberian Peninsula, the largest territory of Southern Europe with a Mediterranean climate characterized by a hydrological deficit year around, particularly critical during the dry and hot summers.

Water availability and soil erosion have been recognized as the most significant environmental problems in the Iberian Peninsula (García-Ruíz et al., 2013, 2011; López-Moreno et al., 2007; Lorenzo-Lacruz et al., 2010), controlled by both, climate and human activities, as land clearance for crops or grazing, farming and mining developed (Carrión et al., 2010). Soil erosion is related with the absence of protective land cover whereas sediment export to lakes is determined by the onsite sediment production and the connectivity of sediment sources and the lake. The latter factor is also a function of land-use, as the sediment transport capacity is different for distinct types of land-use (Bakker et al., 2008).

Human impact in Iberian landscapes has been particularly intense during the last two millennia (Barreiro-Lostres et al., 2014; Corella et al., 2013; García-Ruíz et al., 2013, 2010; Pèlachs et al., 2009; Roberts et al., 2004). The Iberian Range, located between the Castille Plateau, the Ebro Basin and the Mediterranean coast, provides an excellent case–study for the complex interactions of human activities and climate change in Mediterranean mountain areas at a larger time scales than recent global changes. In this fragile ecosystem, societal and cultural changes have frequently resulted in the collapse of land management systems, higher fire frequency and intensity, and the activation of erosion processes (García-Ruíz et al., 2013). In particular, the evolution of the Iberian Range landscapes has been mainly a history of deforestation, linked with a unique and deep-rooted historical feature: the establishment during Medieval times of a highly complex system of sheep transhumance -the '*Mesta*'- that had intense social and economic implications and a high impact in mountain landscapes (Montserrat Martí, 1992; Pascua, 2012). Furthermore, social factors such as population growth or collapse linked to migrations, wars or large-scale diseases have a large impact on the intensity of soil conservation works in mountain areas, with large environmental implications in the landscape (Esteban Cava, 1994; García-Ruíz et al., 2013; Valbuena-Carabaña et al., 2010). Finally, the 20$^{th}$ century witnessed some of the largest changes in the Iberian Range, as most rivers were regulated (Lorenzo-Lacruz et al., 2010), and after the 1950s, rural mountain areas were abandoned and population pressure greatly decreased, resulting in lower soil erosion due to vegetation recolonization (García-Ruíz et al., 2013).

In the Mediterranean region, lake sediments have been shown to be exceptional archives of past environmental and climatic evolution at the regional scale (see Lionello, 2012; Magny et al., 2013; Moreno et al., 2012; Roberts et al., 2012). In the Iberian Range, due to the dominant carbonate

nature of the rock formations, most of the lakes are of karstic origin (Valero-Garcés and Moreno, 2011). Although both lake basins and watersheds are relatively small, intense depositional processes commonly leads to high sedimentation rates and thick deposits, providing long continuous sedimentary sequences with a high temporal resolution and an exceptional sensitivity to both regional hydrological balances and human induced land-use changes (Valero-Garcés et al., 2014). As observed by Dearing and Jones (2002), small lakes draining small-medium catchments (< 1000 $Km^2$) provide the largest number of sediment flux palaeorecords, from a variety of climatic zones. These studies also showed that during the Late Holocene, climate has been largely subordinate to human impact as main controller of long-term shifts in sediment loads, though the evidence for intense impacts from short-term climatic phases is also abundant. Small basins are most responsive to external impacts and will show the largest changes in sediment flux.

In this paper, we investigate the evolution of El Tobar Lake and its watershed during the last millennium using a multi-proxy analysis of the sediment sequence and historical and documentary data. The objectives of this study are: i) to reconstruct the main depositional phases in the lake, particularly sediment delivery fluctuations, and ii) to explore the relationships between these sediment delivery dynamics and natural (climate) or anthropic (land use changes) forcings. The results provide a general framework for the recent hydrological and land use changes in the region and long-term data to evaluate local and regional management policies.

## 2. The Iberian Range: climate, landscapes and human activities

### *2.1. The study area*

El Tobar Lake (40°32′N, 3°56′W; 1200 m a.s.l.) is located in the *Serranía de Cuenca* (Western Branch of the Iberian Range), at the headwaters of the Tagus River (figure 1A). Jurassic and Cretaceous carbonatic formations dominate in the region, and karstic processes are main geomorphic agents (figure 1B). They led to the formation of lake basins behind travertine dams e.g., Lake Taravilla (40º39′N, 1º58′W, 1100 m a.s.l., Moreno et al., 2008) and in flooded sinkholes, as occurs in the seven karstic lakes of Cañada del Hoyo (39ºN, 1º52′W, 1000 m a.s.l., Barreiro et al., 2014) and also in El Tobar Lake (Vicente et al., 1993).
The watershed, although relatively small, is one of the largest in the region (1080 ha surface area) and is drained by several ephemeral creeks. The low altitude areas (~1100 m.a.s.l.) of the watershed are carved in easily erodible materials (Upper Triassic Keuper facies, composed by mudstones and gypsum rocks). Keuper facies act as an impermeable layer sealing the base of the Jurassic and Cretaceous regional aquifer. The limestones and dolostones formations dominate the catchment highlands (~1400 m.a.s.l.). A number of sinkholes occur in the watershed, likely developed by dissolution of the evaporitic Keuper facies and the overlying Jurassic and Cretaceous limestones and dolostones formations, that have been also affected by gypsum-driven dedolomitization karstification processes (Bischoff et al., 1994).

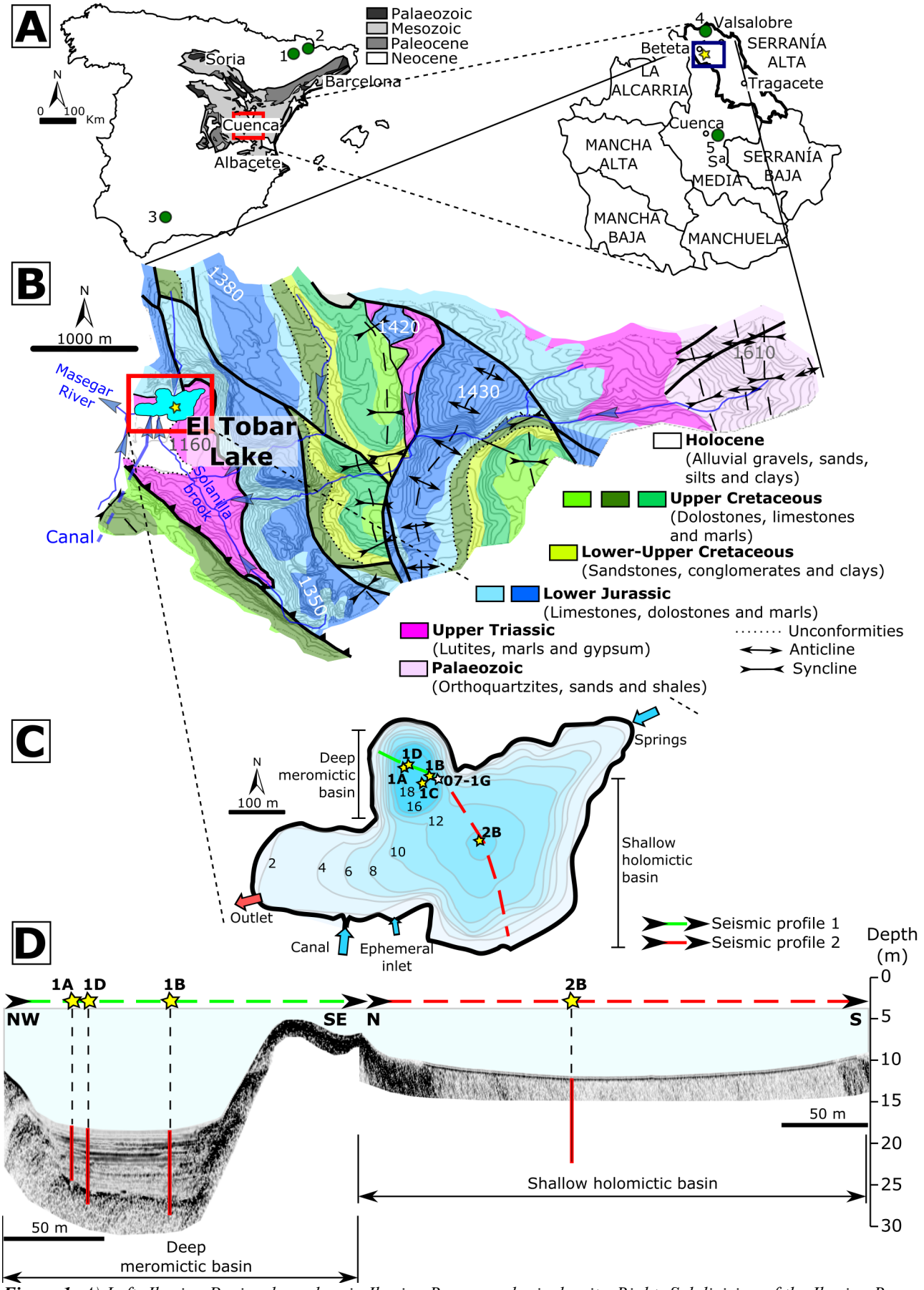


***Figure 1**: A) Left: Iberian Peninsula and main Iberian Range geological units. Right: Subdivision of the Iberian Range in the study area: Serranía Alta, Media and Baja. Green dots represent the locations of main regional records in the Eastern Iberian Peninsula discussed in text: Pyrenees (1, Estaña, 2, Montcortès), South (3, Zoñar) and Iberian Range (4, Taravilla, 5, Cañada del Hoyo). C) Bathymetric map of El Tobar Lake showing the main water inlets and outlets*

*and the geometry of the small meromictic sub-basin and the large holomictic sub-basin. Number indicates the depth of the isobaths in meters. Yellow stars indicate the position of the recovered long-cores, while white star mark the collected $^{210}$Pb-$^{137}$Cs short-core. Green and red dashed lines indicate the trace of the seismic survey in the deep and shallow basins respectively. D) Seismic lines from the deep sub-basin (green dashed line) and from the shallow sub-basin (red dashed line) and the location of coring sites.*

### *2.2 Modern climate and vegetation*

According to nearby meteorological stations (Beteta, 4 km NW, for the rainfall period 1945-2011 and Cañizares, 20 km SW, for the temperature period 1951-2010), the area has a Mediterranean climate, although modulated by continental influences, with harsh long winters (3 ºC mean monthly temperature) and hot short summers (19 ºC) (figure 1B). Average annual precipitation is relatively high (956 mm) mostly controlled by the westerly winds associated with cold fronts in late fall and winter, but inter-annual variability is large. July and August are the driest months and December the wettest, but during summer and at the beginning of the fall, highly convective storms typically occur. Meteorological records show a small mean annual temperature increase (~2 ºC) and a significant mean annual precipitation decrease since 1980s Current Era (CE), from 1600-1200 to 1000-800 mm.

Vegetation in the El Tobar watershed belongs to the supra Mediterranean sub-humid type with Central Europe tendency (Peinado-Lorca and Martínez-Parras, 1987). Pine trees dominate, with *Pinus nigra salzmannii*, *Pinus sylvestris* and *Pinus pinaster* as the main species; *Quercus ilex rotundifolia, Quercus faginea, Juniperus faginea* and *Juniperus communis* are also present as secondary species in the sunny slopes. Abandoned cereal fields occur at lower watershed elevations and abandoned *Salix* crops, used in the past for an artisan industry, surround the southern lakeshore.

### *2.3 The El Tobar Lake*

El Tobar Lake is the largest karstic lake in the region, with a surface area of 16 ha, and a maximum depth of 20 m. It is divided into two sub-basins (figure 1C): (i) a smaller funnel-shaped, deeper (2 ha, 20 m depth) meromictic basin with an anoxic hypersaline hypolimnion (NaCl, brine, TDS = 19116 ppm), and (ii) a larger shallower holomictic basin (12 m depth, 14 ha) with fresher waters (TDS = 408 ppm) (López-Blanco et al., 2011b; Miracle et al., 1992; Vicente et al., 1993; Vicente and Miracle, 1988). The hypolimnion waters are dominated by $Cl^-$ (305 meq/L) and $Na^+$ (261 meq/L) with pH = 7.6, while in the epilimnion these concentrations decrease until 1.7 and 1.9 meq/L respectively, with higher $CO_3^{2-}$ (3.7 meq/L) and pH = 8.3. The lake is hydrologically open, with subaquatic spring inlets in the eastern shore (TDS= 428 ppm; pH = 7.7) and ephemeral inlets (pH = 8.2) from a small brook (Valle Solanilla creek) in the southern shore. In 1967 a connection with the nearby La Tosca reservoir (3 km southwest, fed by the Cuervo River) was established by an underground canal and since then El Tobar acts as a regulatory water reservoir (Esteban Cava, 1994). This canal provides the freshest waters (TDS = 268 ppm) dominated by $CO_3^{2-}$ (3.6 meq/L) and $Ca^{2+}$ (1.4 meq/L) and $Mg^{2+}$ (0.9 meq/L). The only surface outlet is the Masegar River, a tributary of the Guadiela River. A quantitative water balance for the lake is not available, but groundwater and the artificial canal are the main inputs. Subaquatic springs and ephemeral inlet waters have similar compositions to epilimnetic waters (IPE laboratory measures, not shown). However, the occurrence of a stable hypersaline hypolimnion suggests an active groundwater input from saline spring draining evaporitic Keuper facies (Vicente et al., 1993).

## 3. Materials and methods

### *3.1 Compilation of historical documents*

In Spain, documentary evidence since medieval times is abundant, although in sparsely populated areas such as the headwaters of the Tagus River, information is scarcer. For our purposes we have used some recent compilations as Esteban Cava (1994) and the review of Valbuena-Carabaña et al. (2010). Both provide an integrated and dynamic account of the evolution of the geographical landscape, the socio-territorial, industrial and economic changes in this area for the last millennium.

### *3.2 Bathymetric and seismic survey*

A bathymetric map from El Tobar Lake was obtained by using a SonarMite echosound connected to a DGPS. A total of 42 N-S and E-W depth-transects with a total length of 9 km were processed with the hydrographic software HYPACK, providing the bathymetry shown in figure 1C. Maximum depths of 19.5 and 13 m were found respectively in the deep and shallow sub-basins.
The seismic survey was conducted with an Edgetech 424-SB sub-bottom multi-frequency profiler using a frequency range of 2-10 kHz for 20 ms. A total of 5.8 km distributed in 24 seismic profiles were obtained. Penetration was very limited in the shallow sub-basin (0.5 m) but reached up to 8 m in the deep sub-basin. Seismic processing workshop software (EdgeTech Discover SB3200 XS) was used for the processing of the pinger data (bandpass filter, flat gain). Two of the seismic profiles with the best resolution and penetration have been selected to characterize the main structure of the sedimentary sequence (figure 1D).

### *3.3 Sedimentology and geochemistry*

Four parallel piston cores (TOB04-1A-1K, 5.4 m; TOB04-1B-1K, 7.7 m; TOB04-1C-1K, 7.4 m and TOB04-1D-1K, 7.5 m) were recovered in the deepest part of the deep lake sub-basin (20 m); and one in the shallow sub-basin (TOB04-2B-1K, 7.1 m) with the Limnological Research Center (LRC, Univ. of Minnesota, US-MN) floating-platform, equipped with a Kullemberg piston corer. In 2007, a short gravity core (TOB07-1A-1G, 52 cm) and its replica were retrieved with the UWITEC gravity corer for $^{210}$Pb and $^{137}$Cs dating assays in the deep subbasin.

The piston cores were scanned for sediment gamma density (ρ) and magnetic susceptibility (MS) at 1 and 0.5 cm of resolution respectively, with the Geotek Multisensor Core Logger (MSCL) from the LRC. Then were split longitudinally and imaged with the GEOTEK attached CCD camera at 10 pixel/mm. Sedimentary facies were described following the methodology established by Schnurrenberger et al. (2003), including smear slides microscope observations. A composite sequence was obtained (Supplementary information figure A1) correlating all cores using distinctive sedimentary facies and MS values.
Two main types of geochemical analyses were performed in the main cores TOB04-1B-1K, TOB04-1D-1K-2, TOB07-1A-1G (deep sub-basin) and TOB04-2B-1K (shallow sub-basin): (i) ITRAX X-ray Fluorescence (XRF) scanner at the University of Minnesota, Duluth (US-MN) at 0.5 mm of resolution with a Mo tube under the following working conditions: 30 kV, 20 mA and 30 s of exposition time per measurement point; and (ii) 53 samples covering all sedimentary facies, for quantitative elemental assays of major and trace elements by Inductively Coupled Plasma-Mass Spectrometry (ICP-MS), using a Perkin/Elmer Nexion 300X ICP-MS at the University of Pittsburgh (US-PA), following Pompeani et al. (2013). This double approach enables a complete geochemical description for each facies. The L* value calculated with ImageJ 1.48v graphic software (http://imagej.nih.gov/ij/) applied to X-Ray (XR) images obtained by the ITRAX XRF scanner was used to identify the light, gray and dark laminae occurring in the laminated facies.
The cores were also sub-sampled every 2 cm for Total Organic (TOC) and Total Inorganic (TIC) Carbon, and every 4 cm for Total Nitrogen (TN). TIC and TOC were measured with a LECO SC144DR and TN with a VARIO MAX CN elemental analyzer from the Instituto Pirenaico de Ecología (IPE-CSIC, Spain).

Mineralogy was determined on selected samples covering all facies variability by a Siemens D-500 X-ray diffractometer (Cu kα, 40 kV, 30 mA, graphite monocromator) at the Serveis Científico-Tècnics of the ICTJA-CSIC (Spain). Identification and relative abundance of the predominant mineralogy of the crystalline fraction were determined following Chung (1974a, b). Three samples from each sedimentary facies were analyzed for grain-size distribution using a Beckmann Coulter LS 13 320 Particle Size Analyzer and facies were classified using the Shepard diagram (Shepard, 1954).

The relationships among the geochemical and sedimentological signals were investigated with Principal Component Analysis (PCA) applied to a dataset including LECO, XRF and facies data. Only the elements with a mean XRF counts per second (cps) > 1500 have been taken into account to maximize the quality of the interpretations. Then XRF data was re-sampled from the original resolution of 0.5 mm to 2 cm (LECO resolution) to compare both datasets. A final dataset with 12 variables per 359 samples was constructed and a Principal Component Analysis (PCA) was carried out using the R software 3.2.0 (R Development Core Team, 2015) with the package FactoMineR 1.29 (Lê et al., 2008).

### *3.4 Chronology*

The construction of the age-model for El Tobar sequence has been a long and iterative process that involved different types of samples and techniques (see Table 1). Firstly, three wood macrorests were dated soon after the cores were retrieved (two *Salix sp*. at 551 and 789 cm depth, and one sample species not identified at 765 cm). As the results were contradictory, and no more macrorests were found in the sequence, we look for macro-charcoals, and although their presence in the sediments also was scarce, three samples (472, 756 and 768 cm depth) were dated. Finally, in a third attempt to improve the age-model and due to the scarcity of wood or charcoal fragments, bulk sediment (one sample at 789 cm depth) and pollen concentrates (three samples at 206, 279, and 507 cm depth) were also dated. Three different laboratories have been involved in dating the 10 samples from core TOB04-1B-1K: the Poznan Radiocarbon Laboratory (Poland), the DirectAMS Laboratory (US-WA) and the Quaternary Dating Research Unit Laboratory from the Council for Scientific and Industrial Research (South Africa). Radiocarbon dates were calibrated using the curve IntCal 13 (Reimer et al. 2013) and selecting the median of the 95.4% distribution (2σ probability interval).

***Table 1:*** *Radiocarbon dates used for the construction of the age model for El Tobar sequence. Dates were calibrated using Clam 2.2 software (Blaauw, 2010) and the IntCal13 curve (Reimer et al., 2013). The 2 σ probability interval was selected. Dates with * were discarded (reversals or stratigraphically inconsistent).*

| Composite core depth (cm) | Laboratory code | $^{14}$C AMS age (BP) | 2σ calibrated age (cal. year. AD/BC) | Material |
|---|---|---|---|---|
| 206 | Liv-155626 | 1070 ± 80 | 915 ± 144* | Pollen |
| 279 | Liv-155626 | 2055 ± 40 | -75 ± 101* | Pollen |
| 472 | Liv-155624 | 140 ± 30 | 1844 ± 46 | Charcoal |
| 507 | Liv-155628 | 1425 ± 45 | 610 ± 57* | Pollen |
| 551 | GrA-28169 | 750 ± 40 | 1254 ± 45* | Wood (Salix) |
| 756 | Liv-155625 | 560 ± 35 | 1335 ± 30 | Charcoal |
| 765 | GrA-28170 | 695 ± 40 | 1289 ± 33 | Wood fragment |
| 768 | Liv-153057 | 890 ± 35 | 1167 ± 51 | Charcoal |
| 789 | Poz-12365 | 2050 ± 30 | -53 ± 70 * | Bulk sediment |
| 789 | Poz-12233 | 410 ± 30 | 1476 ± 44* | Wood (Salix) |

The uppermost sediments of the sequence were recovered in the short core TOB07-1A-1G and correlated with the uppermost part of the TOB04-1B-1K long core using TOC values. $^{137}$Cs and $^{210}$Pb profiles were obtained in the short core by gamma ray spectrometry at the St. Croix Watershed Research Station (US-MN). The $^{210}$Pb dates were determined following Appleby (2001). A final age-depth model based on four $^{14}$C dates and the $^{137}$Cs peak was performed with Clam 2.2 code (Blaauw, 2010). The final curve, after different fits with other regression models, was adjusted with a degree 3 polynomial regression, which provided the best-fitting curve for the dates.

## 4. Results

### *4.1 The sediment sequence*

The NW-SE seismic profile shows well-defined reflections of alternating high and low amplitude, likely correlating with density contrasts caused by alternating sedimentary facies along the deep sub-basin (figure 1D). In the central part of the basin where the cores were retrieved, the seismic survey confirms that the sediment sequence is continuous, and not affected by large mass wasting processes. In the western margin, well - defined reflectors show an onlap structure at the top that could be related to relatively higher lake levels in the recent past. In the eastern margin, reflectors in the upper half of the sequence are chaotic and discontinuous. Thus, the occurrence of mass wasting

deposits associated to slope instability, a common process in relatively deep, sinkhole lakes (Corella et al., 2014; Morellón et al., 2008) is very limited in El Tobar and restricted to the eastern margin.

Visual sediment description of structures, textures and composition, smear slide observations, mineralogical analyses, grain size and geochemical composition (both elemental and XRF) allowed the identification and characterization of seven facies in the El Tobar composite sequence. The base of the sequence (795-770 cm depth) is composed by **facies 1** (brown sandy silts) **and 2** (gray sandy silts), both with abundant terrestrial plant and gastropod fragments. Above them, **facies 3** (black massive sandy silts) only occurs in this interval (770-750 cm depth). Facies 1, 2 and 3 have <20% of quartz and clay minerals, between 30 and 45% of calcite and between 20 and 50% of dolomite (see figure 2). The upper 750 cm of the sequence consists of an alternation of laminated light (**facies 5**), gray (**facies 6**) and dark (**facies 7**) clayey silts. Facies 6 and 7 are finer, with higher clay content (> 40 %) and with more abundant diatoms relative to facies 5 (figure 2). Facies 5 shows more frequent soil oxidized agglomerates and higher dolomite content (20%) than in facies 6 and 7 (~12%). Massive, light-colored sandy silt layers (**facies 4**) interspersed in the laminated sequence. They occur as 10-40 cm thick, homogeneous layers with no apparent grain-size gradation that can be correlated among all cores recovered in the both shallow and deep subbasins. Grain size analyses indicate they are coarser than facies 5, 6 and 7 (clayey silts) and they contain more dolomite (>30%) and less clays than facies 5.

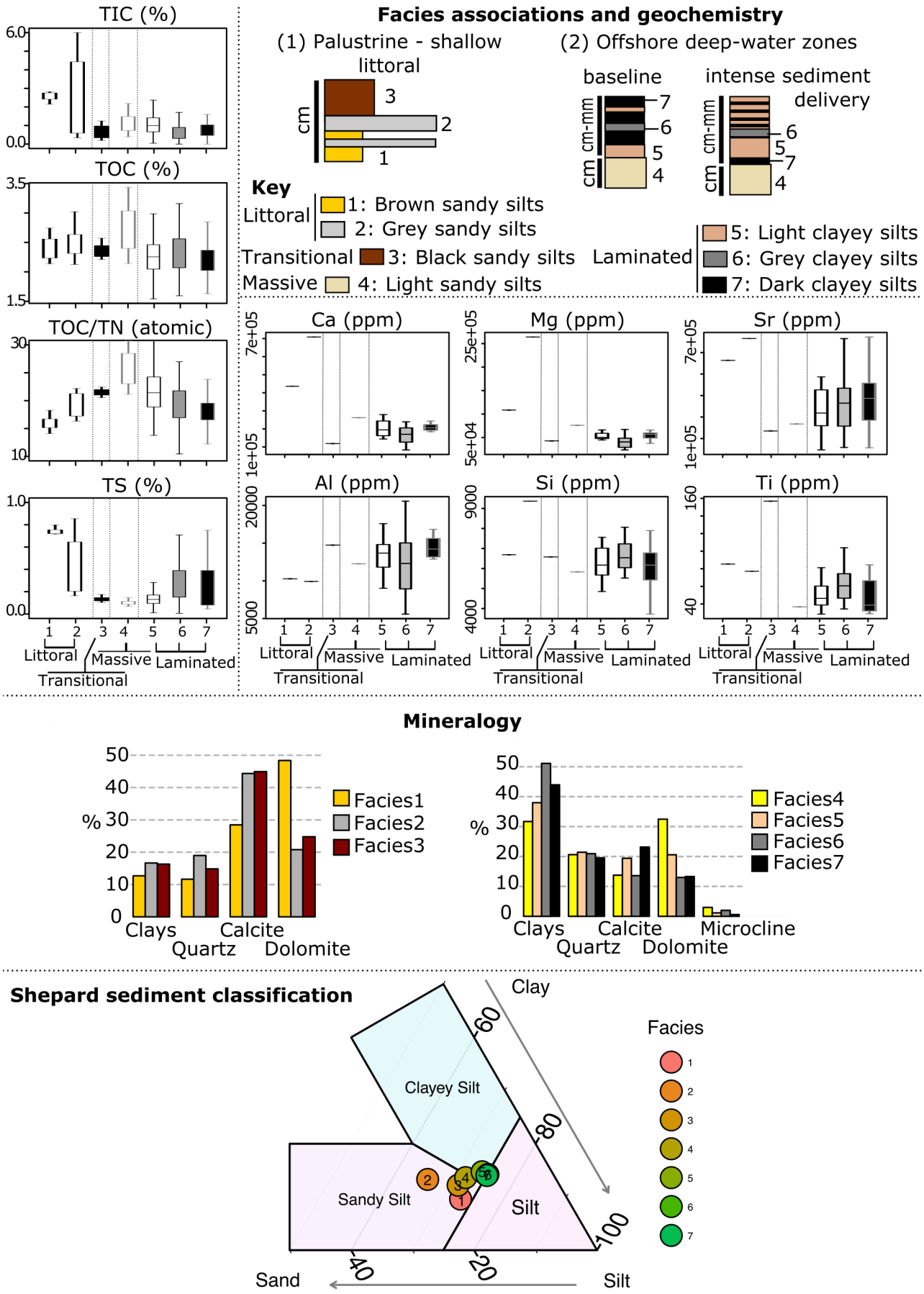


***Figure 2:*** *Main facies associations (top) and geochemical box-plots for TIC (%), TOC (%), TOC/TN (atomic) and TS (%) values (top left side) and main geochemical composition (ICP values, top right side) categorized by facies. Also XRD mineralogical analysis (middle) and textural composition of facies (bottom) are shown.*

The El Tobar sediment record is organized in six sedimentary units composed of finning-upward sequences (figure 3A). The basal **unit VI** (795-770 cm) includes facies 1 and 2. **Unit V** (770-670 cm) starts with the deposition facies 3. It is followed by gray and dark laminated facies (6 and 7) with progressively more frequent light laminated silts (facies 5) towards the top. **Units IV to I** (670-0 cm) show the same internal depositional structure (Figure 3A): relatively coarser light colored silts (facies 5) at the base grading into more frequent finer, darker laminated silts towards the top (facies 6 and 7). The base of each unit is defined by the occurrence of thick layers (10-20 cm) of massive light silts (facies 4). The upper **Unit I** has been subdivided into **subunit Ib** (180-40 cm) dominated by light facies 5 and **subunit Ia** (40-0 cm) dominated by dark facies 7.
Magnetic susceptibility (MS) shows a decreasing trend from unit V (770 cm) to Ib (40 cm) (figure 3A). MS shows a large variability range along units, however light massive facies 4 at the base of each unit and light laminated facies 5, (low XR L* color values) have relatively higher values, than dark laminated facies 6 and 7 (high XR L* color values).

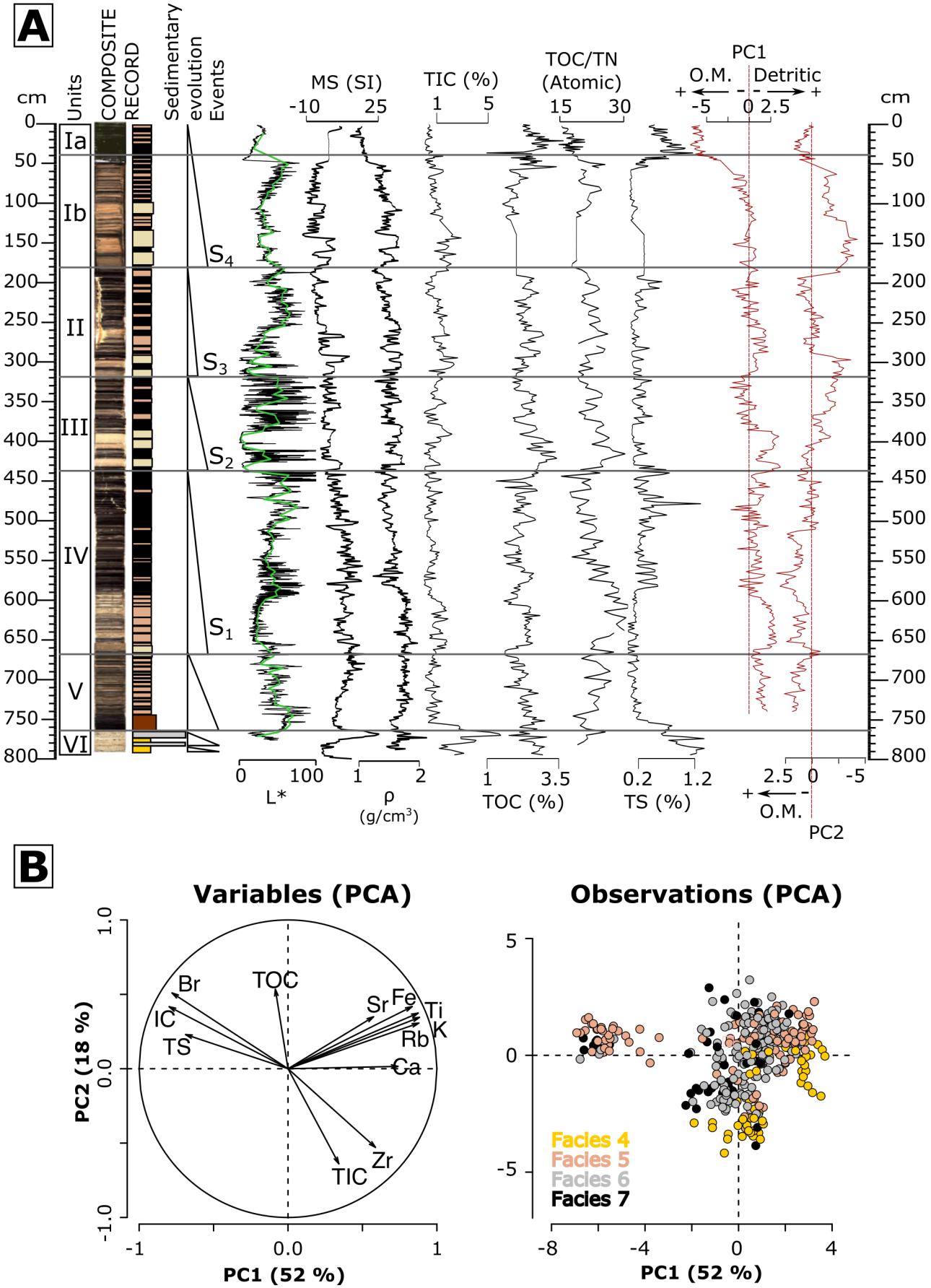


***Figure 3:*** *A) Composite sedimentary sequence from El Tobar. From left to right: units, core image, sediment stratigraphy, facies with sedimentary evolution organized in fining-upward sequences and sedimentary events, Llightness (L*), magnetic susceptibility (MS [SI]), density (ρ [g/cm$^3$]), basic geochemistry TIC (%), TOC (%), TOC/TN (atomic) and TS (%), and PC1 and PC2 eigenvectors (plotted in red) summarizing geochemical XRF stratigraphy. B)*

*Left: Principal Component Analysis (PCA) of El Tobar composite record using main geochemical XRF elements, elemental composition (TOC, TIC, TS), incoherence/coherence ratio (IC). The first eigenvector (PC1) highlights the detrital inputs, whereas the second eigenvector (PC2) is interpreted as changes in organic content. Right: Map of the facies distribution.*

### *4.2 Geochemistry*

Facies 1 and 2 have a distinctive composition compared to the rest. They present relatively higher TIC, TS, Ca, Mg and Sr (see figure 2). On the other hand, facies 4, 5, 6 and 7 have a similar composition, with only small geochemical differences. Facies 4 presents relatively higher TOC, TOC/TN and Ca and Mg compared to Facies 5, 6 and 7 that cannot be geochemically differentiated among them. Facies 3 has a geochemical signal similar to the composition of facies 4, 5, 6 and 7 but with relatively higher Al and Ti.

TIC values range between 1-5%, except for dark massive facies 3 (770-750 cm) where they reach ~3-6%. Although the values are similar from units V to I (figure 3A) they show an internal structure with higher values at the base of each unit and lower towards the top, following the finning-upward structure of each unit. The Ca and Mg contents in El Tobar sediments are relatively high, as usually occur in carbonate watersheds (see figure 1C). TOC present higher values in light laminated facies (facies 5) than in homogeneous facies 4. The highest values are reached in subunit Ia. TOC/TN values in El Tobar range between 15 and 30, and follow a similar trend as TOC. TS curve shows the highest values in facies 1 and 2 (unit VI, 795-770 cm; ~0.5-1%) and moderate values in facies 3 (unit V, 770-750 cm; ~0.5%) and from 60 to 25 cm depth (top of unit Ib and base of unit Ia). In general, TS has relatively lower values in light laminated facies and higher values in dark laminated facies.

The PCA integrating Incoherence/Coherence ratio (IC), TOC, TIC, TS and XRF geochemical variables (figure 3B left) identified three end members. The first one is positively correlated to the first principal component (PC1 axis, 52% of the variance) of the PCA presenting high positive loadings for Sr, Fe, Ti, K, Rb and Ca. The second pool has positive loading for the first principal component and negative loadings for the second principal component (PC2, 18% of the variance) and includes TIC and Zr. The third end member is positively correlated with the second principal component (PC2 axis) and negatively with the PC1 and includes TOC, Incoherence/Coherence ratio (IC), Br and TS.

The addition of the sedimentological information allows mapping the distribution of the geochemical data according to facies (figure 3B right). The distribution of observations along negative PC1 values (affecting mainly facies 6 and 7) corresponds with individuals from the short core TOB07-1A-1G and this could be an artifact caused by higher water content in the sediments. The plot shows that facies 5, 6 and 7 have a similar geochemical signature, positively correlated with Sr, Fe, Ti, K, Rb and Ca; facies 5 is relatively stronger correlated with the last end members and facies 7 although has a high distribution range, presents a higher correlation with the geochemical elements related to the presence of organic matter (TOC, IC, Br and TS; negative PC1 and negative PC2 scores). Facies 4 is strongly correlated with Ca, TIC and Zr (positive PC1 and negative PC2 scores) and shows no correlation with organic proxies.

PC1 presents high values at the base of unit IV (650-600 cm), III (430-380 cm), II (310-250 cm) and Ib (180-150 cm). PC2 follows a general decreasing tendency from units V to Ib (figure 3A) with the highest values in unit V (730-670 cm), V (650-510 cm), top of unit II (230-200 cm) and unit Ia (40-0 cm).

The composition of light, gray and dark laminated facies (5, 6 and 7), which make most of El Tobar record, has been investigated using Ti and Br/Ti and Ca/Ti ratios from semiquantitative XRF

analyses at 0.5 mm resolution (supplementary material figure A2). The three types of laminae show small differences in geochemical composition and they follow similar patterns along the record.

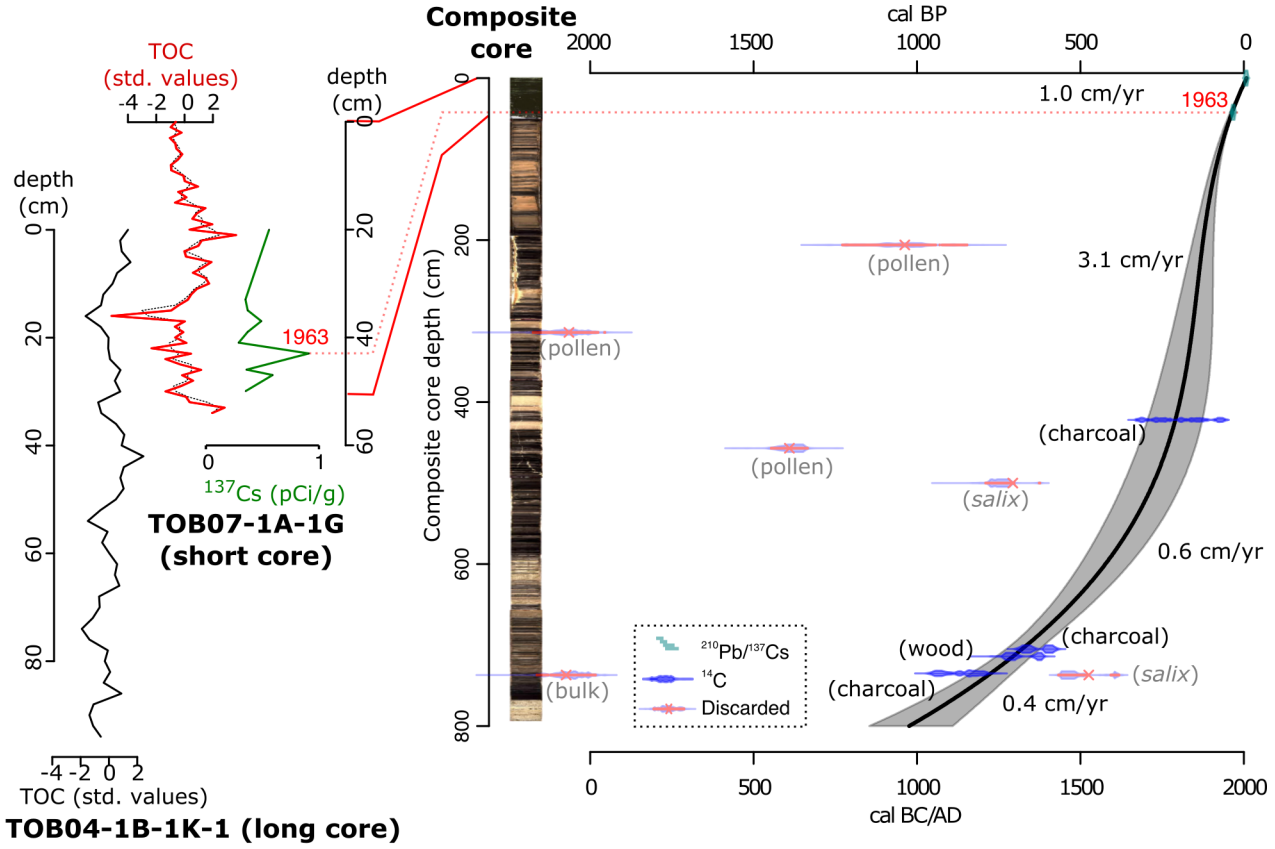


***Figure 4:*** *Left:* Correlation using TOC (%) standardized values between the short core with $^{137}$Cs dates (red line, gray dotted line represents the smoothed curve) and the long-core (black line) with $^{14}$C dates. Right: Age-Depth model of El Tobar sequence based on four AMS $^{14}$C dates from the TOB04-1B-1K long core (blue horizontal lines) and $^{137}$Cs essays (topmost green points) from the short-core TOB07-1A-1G using a weighted spline regression (Blaauw, 2010). Red crossed dates have not been included in the model. Black line represents the age-depth function framed by error lines (gray shaded area).

### *4.3 Chronological model*

Although 10 AMS $^{14}$C dates were obtained, the chronological model for El Tobar Lake sequence is based on the $^{137}$Cs peak date from the short gravity core TOB07-1A-1G and four $^{14}$C dates from the TOB04-1B-1K long core (figure 4)..

We use several criteria to select samples for the final age-model. $^{210}$Pb techniques were employed to date the short core, but as López-Blanco et al. (2011b) also observed, $^{210}$Pb essays show a rather constant and relatively low radioisotope activity along most part of the core, with no clear decreasing values and thus no age-depth relationship can be modeled from this profile. This pattern can be due to both, physical sediment mixing or chemical remobilization processes in the surficial sediment layers (Appleby, 1998).

The exclusion of the $^{14}$C bulk sediment sample (Table 1) is due to its extremely old date, which may be explained by mechanical contamination (i.e. sediment reworking). Moreover, a reservoir effect could affect lacustrine organic matter, also causing older ages. Reworking of older sediments is also an explanation for too old dates provided by wood macrorests. The *Salix sp*. from 551 cm depth was discarded in the age-model because the date is also too old, and incompatible with our final model (figure 4). We also excluded the *Salix sp*. sample from the bottom of the core (789 cm depth) because it provided a rejuvenate date in our age-model. Wood samples, considered

traditionally excellent dating material, may also provide too young dates. As Goh (1991) shows, although wood does not exchange readily with contemporary carbon, woods buried anaerobically under natural conditions in the sediments when excavated and exposed to the air may exchange with atmospheric $CO_2$ and introduce young carbon into the sample. Exchanges of carbon between the sample and the atmosphere are a common cause of contamination in wood. Therefore, even if woody samples are manipulated carefully, such contaminant sources and processes may be responsible for younger dates.

The three pollen samples have been excluded from the final age-model because they provided old dates (figure 4) and they are not consistent among them. These inconsistencies are likely caused because the dated pollen grains are a mix from different plants (aquatics, submerged, terrestrial) and therefore a source of error for radiocarbon dating.

The $^{137}Cs$ assays provided some extra age constraints to the age model. The $^{137}Cs$ peak at 43 cm depth (1963) of the short core TOB07-1A-1G, corresponding to the 1963 nuclear tests, is in good agreement with the $^{14}C$ date model (figure 4). Moreover, the sedimentation rate provided by the $^{137}Cs$ essay gives a rate of 1 cm/year of the topmost 50 cm, which is in agreement with the sedimentation rate (0.8 cm/year) get from the $^{14}C$ for the composite core, constituted by similar lithofacies. A previously dated core (López-Blanco et al., 2011) provided a similar sedimentation rate for the recent sediments.

Therefore, the most simplistic and coherent age-depth model is based on one wood and three charcoal $^{14}C$ dates and is constrained at the top by the 1963 $^{137}Cs$ peak. In spite of the large number of discarded radiocarbon dates, the coherence between $^{14}C$ and $^{137}Cs$ dates strengthen the robustness to this age-model. These results show that the 8 m El Tobar Lake sequence spans the last 1000 years.

## 5. Discussion

### *5.1 Geochemical signature of depositional facies*

The PCA allowed further investigation of depositional and geochemical processes for each facies. The elements that are positively correlated with the PC1 (i.e. Sr, Fe, Ti, K, Rb and Ca; figure 3B) reflect the allochtonous detrital sediment fraction originated in the catchment. Ti, one of the most representative PC1 elements, derives from detrital minerals and is not affected by weathering or diagenetic processes. Also Ti, Rb and K are often associated with clay mineral assemblages (Kylander et al., 2011). Thus, we infer that the positive values of PC1 are representing fine allochtonous detrital sedimentary inputs from the watershed. Therefore, grainsize (higher fine particles content), mineralogy (higher clay mineral content) and PCA results (relatively good correlation with the PC1) point to facies 5, 6 and 7 as dominated by fine-grained sedimentation of detrital material from the watershed.

Both facies 5 and 7 present a subset of samples with higher correlation with the organic-matter end member (TOC, TS, IC, Br) (figure 3B). However, as these samples with extreme negative loadings for PC1 are all from the short core, this distinctive geochemical behavior may be due to higher water content of the topmost section of the composite sequence and not too real geochemical differences. Available ICP values do not show significant differences between recent and older sediments.

Most of facies 5 samples are correlated with positive values of the PC1 and PC2 (detritic related end members). The occurrence of soil oxidized agglomerates and the relatively higher grain size

and moderate amounts of dolomite also point to dominant detrital origin for this facies. Facies 7 although shows a larger dispersion, is correlated to negative PC1 loadings (less detrital). Therefore facies 5 is more dominated by the fine detritic component transported from the catchment, in some cases, relatively rich in organic soils components; facies 7 represents the out of suspension sedimentation, relatively more influenced by the autochthonous lake productivity.

The second pool defined in the PCA (TIC, Zr) is also correlated with the positive values of PC1, suggesting that carbonates in facies 4 are detrital. This interpretation is also supported by the DRX analysis that shows higher calcite and dolomite content in facies 4 likely from the highlands of the catchment, and by microscope observations (large carbonate grains, corroded textures). Zirconium is normally enriched in medium to coarse silts and sand size fraction, and is associated with weathering-resistant heavy minerals like zircon. So, in fine-grained sediments, as those of El Tobar Lake, we would expect to be relatively enriched in the coarser fraction (Kylander et al., 2011), and this would explain the relatively good relationship between clastic carbonates and Zr-bearing minerals. The opposite relationship between TOC and TIC and between TIC and other indicators of organic content (IC, Br) also support that most carbonates in El Tobar are of detrital origin.

Facies 4 is clearly single out in the PCA biplots. It is strongly related with the second pool of geochemical elements (TIC and Zr). Therefore, facies 4 is indicating an allochtonous, relatively coarser sediment, rich in calcite and dolomite grains from the highlands of the catchment.

The third end member (TOC, Incoherence/Coherence ratio (IC), Br and TS) is positively correlated with the second principal component (PC2 axis) and negatively with the PC1. Geochemical (TOC/TN) and microscopic observations are not conclusive whether most of the organic matter in El Tobar laminated facies comes from the catchment or from in-lake productivity. Although TOC/TN values in El Tobar range between 15 and 30, indicative of dominant allochtonous, terrestrial sources (Meyers and Lallier-Vergés, 1999). Microscope observations show terrestrial plan remains occur in the soil oxidized agglomerates of facies 5 and algal matter in facies 7.

### *5.2 Lacustrine depositional processes*

Sedimentological and geochemical features point to a shallow, littoral depositional environment for unit VI. Facies 1 and 2 are composed basically of carbonates (50-90 %) and contain bioclasts (gastropods) and terrestrial plant remains. Large size, irregular and eroded textures confirm a detrital origin for both dolomite and calcite grains. Carbonate endogenic production in El Tobar is very restricted in modern environments; charophyte meadows and encrusted macrophytes areas, common in other karstic lakes, do not occur in El Tobar, so the bioproduction of calcite in this system is small.

At the onset of Unit V, Facies 3 represents a large change in depositional dynamics. Finer darker sediments, with relatively higher TOC and lower TIC, TOC/TN and TS percentages suggest deeper environments with anoxic conditions. The transition between Units VI and V shows no stratigraphic unconformity and deformation structures (folds, microfaults) are absent in both units. Although the absence of macroscopic evidences for slumping does not preclude the occurrence of such processes -e.g., Montcortés Lake (Corella et al., 2011)-, unit V to I shows similar stratigraphy in the deep and shallow basins, and consequently slumping processes can be excluded during deposition of most of El Tobar sequence. This is also supported by the seismic survey showing continuous reflectors all over the deep basin (figure 1D). However, since the core in the shallow basin was not long enough to reach the depths where unit VI could be located in the shallow basin, we cannot rule out that the base of the sequence (790-770 cm, figure 3A) corresponds to a large mass wasting deposit affecting only the deep basin.

If there is stratigraphic continuity between Unit VI and V, this transition was the largest change in the lake during the last millennium, in terms of morphology, hydrology and depositional dynamics: El Tobar Lake shifted from a shallow, well mixed body of water (likely a few meters deep) dominated by littoral carbonate deposition (facies 1 and 2) to a deeper water body with sedimentation of organic-rich facies under suboxic conditions. If the base of the sequence (Unit VI) constitutes a large mass wasting deposit emplaced prior to deposition of unit 3 (ca. 12$^{th}$ century), depositional environments in the NW areas of the Lake would have been similar (deeper, predominantly anoxic) and no significant lake level change would have occurred.
Such a large hydrological change could be related to regional (increase water availability during a more humid period) or local (sinkhole collapse) factors. The onset of deposition of Unit V occurred within the Medieval Climate Anomaly, (MCA), a period generally characterized as a more arid phase in the Iberian Peninsula (Moreno et al., 2012). However there is some evidence of humid phases with increased water availability during the 12$^{th}$ century with increased flooding in the Tagus River (Benito et al., 2003; 2014) and in the Pyrenees (Corella et al., 2012). A small lake level increase in the Lagunillo del Tejo (100 km southwards) (López-Blanco et al., 2011a) and a humid phase in the nearby La Parra Lake (Barreiro-Lostres et al., 2014) are also described at ~1200 CE. On the other hand, in karstic areas, both exokarstic and endokarstic processes lead to the development of new sinkholes, and the enlargement of older ones. These processes are reinforced during wetter periods. Thus, the hypothetic water-level change during 12$^{th}$ century CE could have been a response to higher water availability caused by climatic change, the deepening of the NW subbasin by karstic processes or, more probably, by the synergy of both forcings. Slumping could also have been favored during more active sinkhole subsidence. Since seismic survey in the shallow areas did not show the internal structure due to low penetration, only deeper coring in this basin could help to constrain if unit 6 was deposited in situ or emplaced.

In any case, in this study we focus in the lake evolution after unit 5, characterized by deposition of finer, laminated, more clay-rich facies 5, 6 and 7 with interspersed relatively coarser (sandy silts) facies 4. Laminated facies are geochemically similar, but facies 4 presents relatively higher TOC, TOC/TN and elemental Ca and Mg. Although carbonate content in facies 4 is relatively higher than in laminated facies, the absence of any components typical of shallow littoral facies (1 and 2) as bioclasts, macrophytes or large dolomite and calcite grains do not favor reworking of littoral sediments as a mayor contribution for facies 4. Thus, geochemistry, texture, mineralogy and grain size suggest a relatively different sediment source and depositional process for facies 4 than for facies 5, 6 and 7. Although some small contribution of littoral sediments may occur, the data favor an allochtonous origin (watershed) for most of the sediment. Facies 4 layers can be traced in both the deep and shallow basins cores, so they are not restricted to depositional processes in the deeper areas (for example, associated to slumps; supplementary material figure A1). Facies 4 is thus interpreted as deposited during floods, and not related to mass wasting deposits or debris flows caused by destabilization of the lake slopes.

Although geochemically are very similar (figure 2), facies 6 and 7 present relatively more diatoms and lacustrine organic matter relative to facies 5, where a dilution effect (higher clastic input) could be significant. Higher calcite content and occurrence of small calcite crystal (smear slide observations) in facies 7 also suggest a limited endogenic carbonate production in facies 7. The More frequent soil oxidized agglomerates and the higher content in detritic dolomite (20%) in Facies 5 also favor a relatively higher allochtonous detritic influence than laminated facies 6 and 7. The alternation of facies 5, 6 and 7 is interpreted as baseline “normal” deposition in the lake during the last millennium.

### *5.3 Sediment delivery events*

Since the onset of Unit V (12$^{th}$ century CE), significant depositional changes in the system were

characterized by the intercalation of massive, thick, light-colored coarser sediments (facies 4) over the baseline lake sedimentation (alternation of facies 5, 6, and 7). The input of these materials occurred, from older to younger, during four periods: the end of 16th century CE (unit IV, 650 cm), late 18th century (unit III, 435 cm), mid 19th century (unit II, 325 cm) and beginning 20th century CE (unit Ib, 185 cm) and they have been named consecutively as sedimentary events S1, S2, S3 and S4 (figures 3 and 7).

The geophysical and geochemical signatures of these depositional events (low XR L* color values, high MS and ρ values, high TIC and TOC/TN, low TOC and TS, high PC1 and usually low PC2 values, see figure 3B) are coherent with a higher input of coarse clastic particles (Zr and silicate minerals, iron oxides, carbonates) derived from watershed.

From a sedimentological point of view, the 16th century depositional event S1 is texturally different form the rest, composed of many thin layers of light massive silts (facies 4) and light laminated silts (facies 5) intercalated within dark laminated facies 7. The other events (S2 to S4, 18th-20th centuries) show characteristically a thicker light massive layer of facies 4 with net boundaries at the base of each event.

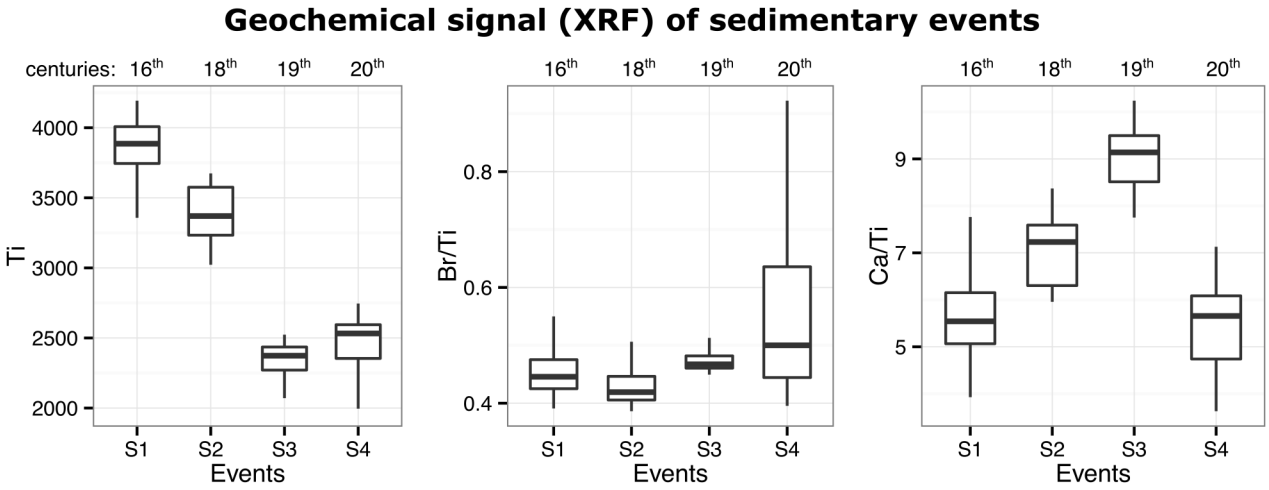


***Figure 5:*** *Geochemical signal of sedimentary events* S1 (16th century) and S2, S3, S4 (18th, 19th, 20th centuries respectively) based on XRF composition (Ti values and Br/Ti and Ca/Ti ratios).

From a geochemical perspective (see figure 5), events S1 (16th century) and S2 (18th century) clearly have more Ti (cps) content than events S3 and S4 (mid 19th and early 20th centuries respectively). Relatively higher Ti content is interpreted as a reflection of more siliciclastic sedimentary inputs from the lake's watershed. Events S1 and S4 present similar Ca/Ti ratios, while events S2 and S3 have the highest values. Higher Ca/Ti ratio is interpreted as more detritic carbonatic sedimentary inputs from the watershed, since productivity of endogenic carbonates, as commented above, is almost negligible.

As the geological sketch from figure 1 shows, the lowlands of the watershed surrounding the lake are constituted by the Triassic Keuper facies, mainly lutites and marls rocks, and they are the principal source for siliciclastic sediments. In the other hand, the highlands of the watershed are dominated by Jurassic and Cretaceous limestones and dolostones and therefore constitute the main source for detritic carbonates. So, considering that endogenic carbonate production is negligible and littoral sediment contributions should be similar in all these events, we hypothesize that changes in Ca/Ti ratio reflect changes in the sediment source – Triassic clay-rich lowlands versus Cretaceous and Jurassic carbonate highlands. A differential use of the landscape through time could explain these changes of sediment source.

### *5.4 El Tobar Lake and watershed evolution during the last millennium*

After the onset of deposition of Unit V (12th century CE), with deeper depositional environments (facies 3), sedimentary dynamics in El Tobar Lake during the next three centuries were relatively stable, characterized by the alternation of facies 5, 6 and 7. The first large change in depositional dynamics occurred at 16th century CE (event S1) when thick, massive light silts were deposited in the basin for the first time. This increase in sediment delivery corresponds with a period of important demographic and economic development in the Serranía de Cuenca, responsible for major pressure over the whole territory (Esteban Cava, 1994). As decreasing crop and anthropogenic taxa percentages from La Cruz record (Burjachs, 1996) show that agriculture became less important in the region from 1200 to 1700 CE (figure 6), and during the 16th century, the progressive deforestation for extensive transhumance stockbreeding reached a peak and changed the Serranía Alta landscape. Many examples suggest a strong relationship between grazing and increased erosion in watersheds in the past. Van der Post et al. (1997) found that recent sedimentation rate rise in the English Lake District was positively correlated with sheep densities in the catchment. Parallel changes have been detected in lakes close to El Tobar during this period (1450-1550 CE): a peak in floods frequency in Lake Taravilla (Moreno et al., 2008); the start of increasing number of floods per decade in the Tagus River at 1560 CE (Benito et al., 2003); higher sediment delivery in Lake La Parra (Barreiro-Lostres et al., 2014); increased deforestation for timber use and livestock grazing at Lagunillo del Tejo and La Cruz Lake (Burjachs, 1996; Julià, 1998; López-Blanco et al., 2011a) (figure 6). So Event S1 in El Tobar clearly reflects regional socio-economic changes that affected the whole area.

Afterwards, depositional dynamics in El Tobar returned to its baseline conditions with dominant dark laminated silts, up to the end of 18th century (upper part of Unit IV). Human pressure in the landscape diminished during this period owing to several demographic and economic crises, mainly due to the Black Death epidemics in 1589 and 1600 CE, and the progressive decrease of the stockbreeding industry. Another phase of increased sediment delivery (event S2) occurred at the end of the 18th century (ca. 1780±86 CE). Although live stockbreeding was greatly reduced at this time, documentary evidence (Esteban Cava, 1994; Valbuena-Carabaña et al., 2010) shows an intensification of new uses of the forest, particularly charcoal for heating and industrial purposes ("*carboneras*") peaking around 1750 CE. Again, other regional records show evidences for forest management, as a local abrupt increase in macrocharcoal at the nearby Lagunillo del Tejo record at 1800 CE (López-Blanco et al., 2011a) and more regionally, an abrupt decrease in *Pinus* pollen from Lake La Cruz (figure 6).

After S2 event and during the first part of the 19th century, sediment delivery decreased again and El Tobar Lake soon regained its previous depositional dynamics. A less intense use of the natural resources at a regional scale is marked by a rapid increase of pine pollen in La Cruz record during this period. This likely reflects the societal convulsions caused by decades of wars. Lower erosion in the watershed was likely due to the abandonment of croplands because of the Napoleonic wars starting at 1800 CE with the French invasion and several Spanish civil wars until 1876 CE (Esteban Cava, 1994; Valbuena-Carabaña et al., 2010).

The next sediment delivery event S3 occurred in the mid-19th century, coetaneous with new expropriation laws in 1855 CE that forced changes in the land property. These new laws dictated the subdivision of large historical estates and infrastructures – some of them historically used communally by the villages – into smaller estates, and favored their ownership by private individuals and entrepreneurs. As a consequence, new wood clearances were practiced without an ordered plan (Esteban Cava, 1994), provoking an increasing pressure in the environment and locally new sources of clastic sediments from the watershed to the lake. The intensity of this event is relatively small compared with previous ones.

After that, a short period returning to lake's baseline sedimentation, by the late 19th century – early 20th century event S4 marks the most intense phase of sediment delivery to the lake in terms of sediment amounts. During this period, population increased all over the Serranía de Cuenca, in conjunction with a new profitable industry based on wood exploitation for building and charcoal production (Esteban Cava, 1994; Lagunillo del Tejo, López-Blanco et al., 2011a) and expansion of farm lands (Lake La Parra, Barreiro-Lostres et al., 2014; López-Blanco et al., 2011a), as shown in the increase of human-related pollen in La Cruz record around this stage (see figure 6), that continued till the mid-20th century.

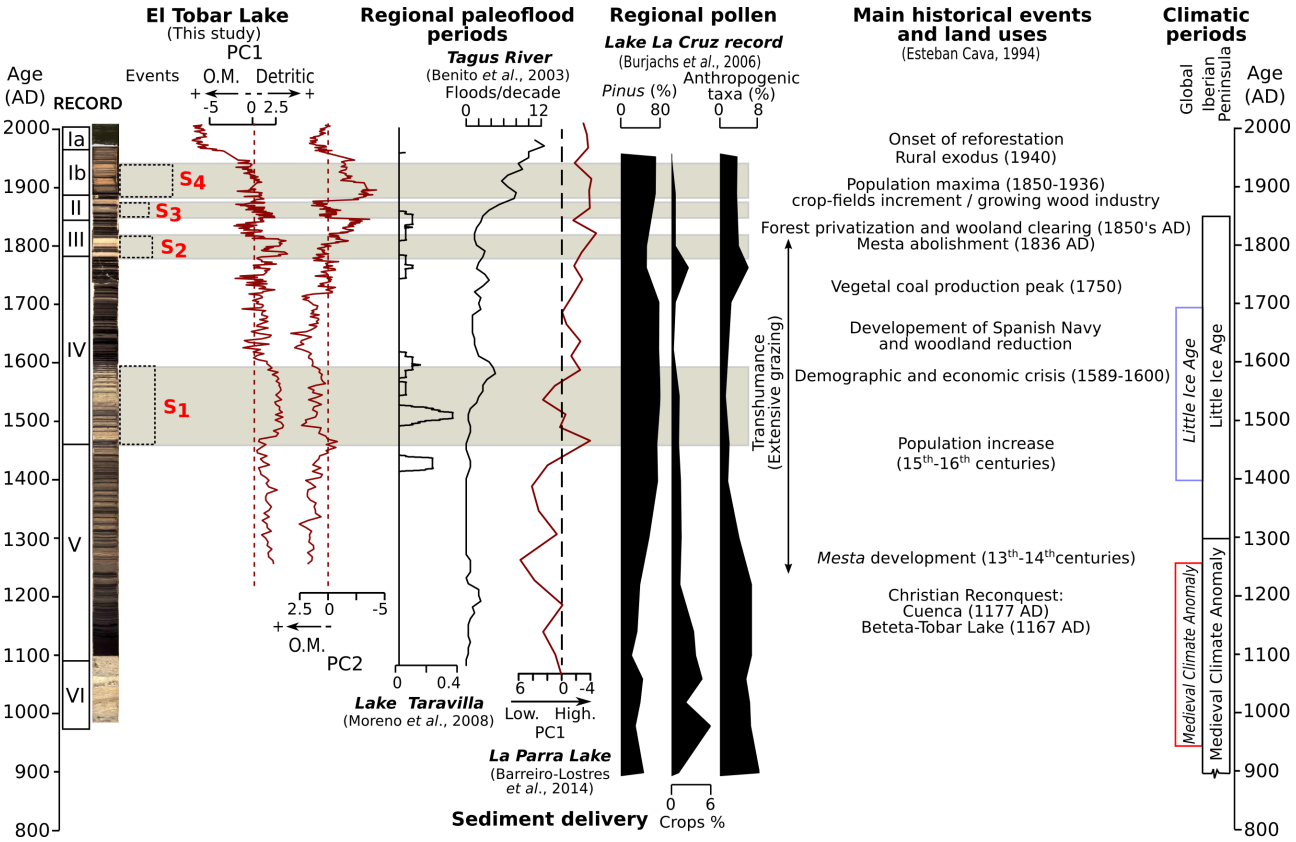


***Figure 6:*** El Tobar Lake depositional evolution during the last 1000 years. Main sedimentary (S1, S2, S3 and S4, brown-shaded) and changes in sediment delivery to the lake (PC1) and sediment organic content (PC2). The El Tobar record is compared with main regional flooding periods reconstructed from Taravilla Lake (Moreno et al., 2008) and Tagus River (Benito et al., 2003) records; and with available regional sequences from the nearby Lake La Parra (sediment delivery, Barreiro-Lostres et al., 2014) and Lake La Cruz (pollen record, Julià et al., 1998) in the Torcas karstic lake complex (see Figure 1 for location). Crops pollen percentage includes *Cerealia, Secale, Cannabacea* and *Vitis*. Anthropogenic pollen taxa include *Artemisia, Plantado, Chenopodia, Brassicace, Urticaceae, Rumex, Centaurea* and *Asteraceae*. Main historical events with large landscape impacts in the study area are also shown. The global North Hemisphere 'Medieval Climate Anomaly' and the 'Little Ice Age' are represented following the chronology of Mann et al. (2009). Chronology for Iberian Peninsula climatic periods is based on Moreno et al. (2012) and Morellón et al. (2011).

In summary, the depositional changes in the record from lower (alternation of facies 5, 6 and 7) to higher (more facies 5) detrital input and, especially the occurrence of periods with much higher sediment delivery (sedimentary events S1, S2, S3, S4 represented by facies 4) are interpreted as a reflection of large change in sediment availability in the watershed and in the energy of sedimentary transport processes (in this case mainly flows and runoff) into the lake. During sedimentary event periods, documentary data indicate that the changes in landscape management due to agriculture and grazing had a strong impact in the watershed. Lower vegetation cover and an intensive land use would have favored an increase in erosion in the watershed and then, most likely, a high influence in the lake sedimentation. From events S1, S2 to event S3 (16th to mid 19th centuries) there is a progressive increase in the Ca content suggestive of higher highland contribution for the sediments

(see figure 5), at same time that occurs the progressive decrease in the powerful stock-breeding industry in the area (figure 6; Esteban Cava, 1994). Event S4 (20th century) has a lower Ca/Ti signal, similar to event S1 (16th century) but relatively higher Ti cps than the previous S3 event. These changes may be attributable to a cropland increment in the lowlands due to a population maximum occurred by 1850 – 1950 CE (Esteban Cava, 1994).

However, climate has also been a significant factor controlling the sediment delivery to the lake. Higher water availability and changing precipitation patterns (seasonality) also affect the sedimentary signal by controlling soil erodibility and sediment transport. The onset of higher sediment delivery periods in El Tobar occurred after 1200 CE, when the first evidence for wetter conditions and higher lake levels after the drier 'Medieval Climate Anomaly' has been documented (~AD 1200) in Lake La Parra (Barreiro-Lostres et al., 2014) and Zoñar (Martín-Puertas et al., 2008). The sedimentary events S1, S2, S3 occur during the wetter and colder 'Little Ice Age'. The S4 event occurs in the late-19th – early 20th centuries during relatively drier conditions, although its magnitude (is the thickest sedimentary event) and documentary data suggest it is likely due to croplands expansion between 1850 and 1936 CE.

Therefore, available sedimentary and documentary data indicate that during historical times in El Tobar Lake, the most intense sedimentary events correlate well with periods of documented high human impact in the landscape. Thus, sediment production is mostly controlled by the human landscape management changes. However, higher precipitation and run off after 1200 CE is the major responsible for an efficient and more intense transport processes in terms of energy and quantity, and thus, the final deposition of the sedimentary events.

After the sedimentary event deposition, the sedimentological and geochemical proxies show a rapid return to the baseline thin-layered sedimentation, without a transitional phase or significant changes in depositional features in the lake. This suggests that in this heavily human-impacted landscape, the depositional and geochemical cycles in the El Tobar Lake, had a high resilience to the variable watershed sediment inputs.

### *5.5. Recent Changes in a long-term perspective*

The present El Tobar watershed landscape is a consequence of centuries of intense human impact and can be considered human-made. Currently, land management is characterized by farmland and grazing abandonment and forest and shrubs expansion as occurs in most Mediterranean mountain areas (García-Ruíz et al., 2011). The farmland abandonment involved a fast and increasing soil degradation of these areas as consequence, for example, of lack of maintenance of the slope bench-terraced fields, leading to new erosional processes (landslides, gullying), that can be dilated in time until shrub colonization. As García-Ruíz et al., (2013) pointed out, these fragile Mediterranean landscapes need the presence of a rural population if they are to be preserved.

Another aspect to consider in the recent evolution of Mediterranean mountain watersheds is the impact of new water infrastructures such as the canal connecting La Tosca reservoir and El Tobar Lake. Although the canal has improved the hydro-power management and facilitated the control of irrigation in downstream areas with increasing human pressure, it led to large modifications in the depositional system as changes in the water composition and lake dynamics and in the ecosystems (López-Blanco et al., 2011b). The canal opening in 1967 CE led to a large hydrological change in the lake, well marked by deposition of dark laminated silts. This depositional change represents a sharp change in the dynamics of relatively high sediment delivery since late 19th century (mainly composed of facies 4 and 5). The canal construction coincided with the peak in depopulation of the area caused by the migration to the cities started during the 1950s. As a consequence, crop-fields were abandoned and during the 1956-1984 period, cultivated area in the watershed was reduced. To

better understand the magnitude of the event and to characterize geochemically the effects of the canal on the lake dynamics, we split the XRF dataset for dark and light lithofacies in unit Ia into two subsets, one pre-canal and another post-canal (pre- and post-1967 respectively; figure 7).

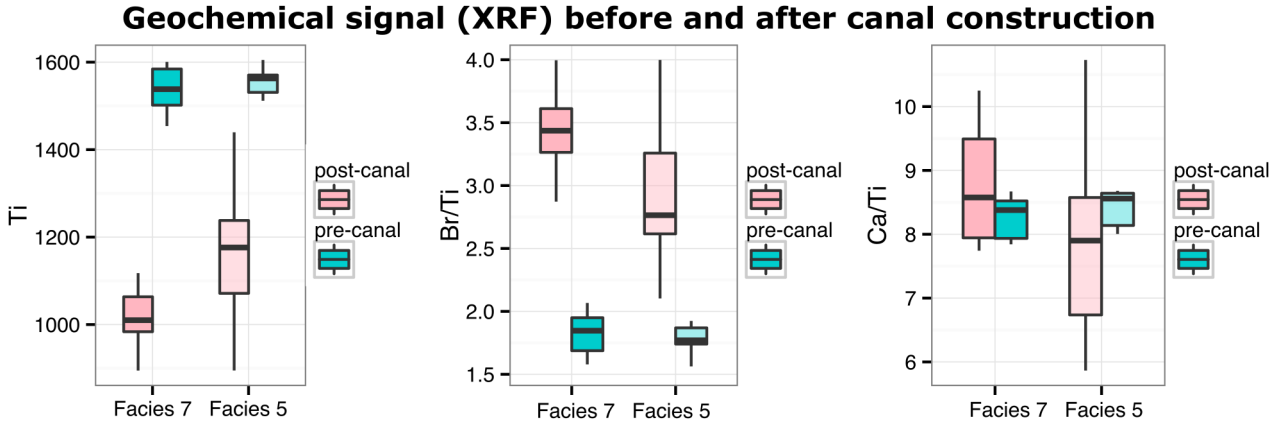


***Figure 7:*** Geochemical signatures of dark and light laminae prior (pre-canal, blue) and after (post-canal, pink) the canal connection of El Tobar Lake with La Tosca Reservoir in 1967.

Although the trends are similar (lower Ti and higher Br/Ti before than after the canal opening), the range of compositional variability is higher in dark laminated facies than in light laminated facies (figure 5). Ca/Ti ratio does not show significant variation in any laminae types. So in the post-canal sediments higher Br/Ti and less Ti, particularly in facies 7, occur. Recent climate variability may have played a role in these changes in lake dynamics. So, deposition of black silts between 1960 and 1980 occurred during a period of higher and more intense rainfall and lower mean temperature (about 2ºC) than during the previous 1984-2010 CE period (Beteta and Cañizares meteorological stations, http://www.aemet.es). Thus, with more frequent rainfalls, likely more nutrients from the recent abandoned valley crop-fields could reach the lake and favor more in-lake organic productivity. A similar pattern has been described in Lake La Cruz (Julià et al., 1998) at the end of the LIA. A shift in Cladoceran assemblages from a dominant benthic to a progressive dominant planktonic composition, taking advantage of a nutrient enrichment, was identified during this period in a separate set of short cores from El Tobar (López-Blanco et al., 2011b). Constant low salinity water input from the reservoir also may change the lake hydrology, increasing lake levels and favoring anoxic conditions on the deep basin due to a stronger chemical gradient. Therefore, the canal opening in 1967 CE led to maintain high lake levels, fresher water inputs and a stronger chemocline. That, coupled with higher nutrient inputs form the watershed provoked a higher in-lake organic productivity and more organic matter preservation in the bottom of the lake, resulting in darker and more organic sediments during the lower half of unit Ia.

After the rapid change caused by the canal opening, in the 1980s the lake seemed to have returned to its previous depositional dynamics (alternation of facies 5 and 7) in a stage characterized by relatively higher sediment input from the watershed. In the upper 20 cm (after 1985 CE), thin laminae of facies 5 are more common. So increased bioproductivity in baseline lake sedimentation occurred at the same time as an increase in the frequency of detrital layers that reflects changes in the watershed (increased storminess, higher availability of sediments).

## 6. Conclusions

The reconstruction of paleoenvironmental conditions based on multi-proxy studies are critical for understanding the dynamics of modern environmental conditions. Thus paleo-limnological approach can contribute to better define the conservation policies for long-time human influenced lacustrine systems and their environment by providing knowledge of their evolution through natural and land-use changes along time.

The geochemical and sedimentological trends identified in El Tobar record, the historical sources of regional land-use and the paleoclimate records allow the reconstruction of the lake-watershed-human interactions during the last millennium in this Iberian Range basin.

Since ca. 1200 CE no major changes in the basin configuration (accommodation space, basin morphology, drainage network) have occurred. The record shows four periods with increased sediment delivery (S1, S2, S3 and S4) that occurred at 16$^{th}$, late 18$^{th}$, mid 19$^{th}$ and early-20$^{th}$ centuries respectively.

The four periods of increased detrital input to El Tobar (S1 to S4) share similar geophysical, geochemical and sedimentological features; and correlate well with the main historical land-use changes in the region, mainly changes in vegetation cover due to large deforestation for grazing, agricultural and farming purposes, favoring erosion and providing sediments for transport by runoff and creeks to the lake. Sedimentologically, the most intense events in terms of sediment amount are S1 and S4, the first one corresponding to the peak in the medieval stockbreeding industry and the later occurring during the period with the highest population in the region. Increased rainfall during some phases of the LIA would have also had a positive synergetic effect with higher anthropic impact in the watershed and cause higher sediment production in the watershed and stronger erosion and delivery.

Interestingly, the transitions in El Tobar Lake from intense to low sediment delivery periods were rapid. Post-event sediments show the same previous undisturbed conditions of lower clastic inputs and relatively higher organic matter and meromictic conditions. The El Tobar Lake has shown a strong depositional resilience to periods of increased sediment influx from the watershed during the last millennium.

This study demonstrates that degradation processes in a mountain watershed such as El Tobar are strongly linked with both natural changes (water availability, flood and runoff frequency) and with anthropic activities (land use changes, soil erosion). Planning conservation strategies of water ecosystems, as El Tobar Lake and surrounding catchment, strongly affected by degradation processes caused by hundreds of years of human activities, should take into consideration the degree of alteration they have experienced and the historical causes of such modifications, leading to site-specific intervention policies over this human-made landscape.

**Acknowledgements**

We want to thank D. Schnurenberger, A. Norens and M. Shapley (Limnological Research Center) for the 2004 field expedition to collect the cores, and the Regional Government (Junta de Comunidades de Castilla–La Mancha) for logistic support. Initial Core Descriptions were performed at the CoreLab (University of Minnesota). F. Burjachs kindly provided pollen data from Lake La Cruz sequence and P. González-Sampériz helped with vegetation dynamics interpretations. S. Vicente nicely provided and elaborated the data from the weather stations. A. Navas and T. Lopez provided quickly the last-minute grain-size analysis. We also thank the numerous colleagues involved in the field campaigns to recover the cores, the LRC, LLO and the University of Pittsburgh staff and IPE-CSIC laboratory services. Authors also like to acknowledge the helpful comments made by reviewers.

This research has been supported by the GLOBALKARST (CGL2009-08415) and GRACCIE – Consolider CSD2007-00067 projects funded by the Spanish Ministry of Economy and Competitiveness and by the I-LINK programme (I-LINK0510) funded by the CSIC. F. Barreiro and

M. Morellón hold ‘JAE-PreDoc’ and ‘JAE-Doc’ pre and postdoctoral contracts respectively, both co-funded by C.S.I.C. and the European Social Fund.

## References

Appleby, P.G., 2001. Chronostratigraphic techniques in recent sediments, in: Last, W.M., Smol, J.P. (Eds.), Tracking Environmental Change Using Lake Sediments, Volume 1: Basin Analysis, Coring, and Chronological Techniques. Kluwer Academic Publishers, Dordrecht, pp. 171–203.

Appleby, P.G., 1998. Dating recent sediments by 210Pb: problems and solutions, in: Proc. 2nd NKS/EKO-1 Seminar. STUK, Helsinki, pp. 7–24.

Bakker, M.M., Govers, G., van Doorn, A., Quetier, F., Chouvardas, D., Rounsevell, M., 2008. The response of soil erosion and sediment export to land-use change in four areas of Europe: The importance of landscape pattern. Geomorphology 98, 213–226. doi:10.1016/j.geomorph.2006.12.027

Barreiro-Lostres, F., Moreno, A., Giralt, S., Caballero, M., Valero-Garces, B., 2014. Climate, palaeohydrology and land use change in the Central Iberian Range over the last 1.6 kyr: The La Parra Lake record. The Holocene 24 (10), 1177 –1192. doi:10.1177/0959683614540960

Benito, G., Macklin, M.G., Zielhofer, C., Jones, A.F., Machado, M.J., 2014. Holocene flooding and climate change in the Mediterranean. CATENA. doi:10.1016/j.catena.2014.11.014

Benito, G., Thorndycraft, V.R., Rico, M., Sánchez-Moya, Y., Sopeña, A., 2008. Palaeoflood and floodplain records from Spain: Evidence for long-term climate variability and environmental changes. Geomorphology 101, 68–77. doi:10.1016/j.geomorph.2008.05.020

Benito, G., Díez-Herrero, A., Fernández de Villalta, M., 2003. Magnitude and frequency of flooding in the tagus basin (central spain) over the last millennium. Climatic Change 58, 171–192. doi:10.1023/A:1023417102053

Bischoff, J.L., Julià, R., Shanks, W.C., Rosenbauer, R.J. 1994. Karstification without carbonic acid: Bedrock dissolution by gypsum-driven dedolomitization. Geology 22, 995-998. doi: 10.1130/0091-7613(1994)022<0995:KWCABD>2.3.CO;2

Blaauw, M., 2010. Methods and code for “classical” age-modelling of radiocarbon sequences. Quaternary Geochronology 5, 512–518. doi:10.1016/j.quageo.2010.01.002

Burjachs, F., 1996. La secuencia palinológica de La Cruz (Cuenca, España), in: Ruíz Zapata, B., Martín Arroyo, T., Valdeolmillos Rodríguez, A., Dorado Valiño, M., Gil García, M.J., Andrade Olalla, A. (Eds.), Estudios Palinológicos. Universidad de Alcalá, Alcalá, pp. 31–36.

Carrión, J.S., Fernández, S., Jiménez-Moreno, G., Fauquette, S., Gil-Romera, G., González-Sampériz, P., et al. 2010. The historical origins of aridity and vegetation degradation in southeastern Spain. Journal of Arid Environments 74, 731–736. doi:10.1016/j.jaridenv.2008.11.014

Chung, F.H., 1974a. Quantitative interpretation of X-ray diffraction patterns of mixtures. I. Matrix-flushing method for quantitative multicomponent analysis. Journal of Applied Crystallography 7, 519–525. doi:10.1107/S0021889874010375

Chung, F.H., 1974b. Quantitative interpretation of X-ray diffraction patterns of mixtures. II. Adiabatic principle of X-ray diffraction analysis of mixtures. Journal of Applied Crystallography 7, 526–531. doi:10.1107/S0021889874010387

Corella, J.P., Benito, G., Rodriguez-Lloveras, X., Brauer, A., Valero-Garcés, B.L., 2014. Annually-resolved lake record of extreme hydro-meteorological events since AD 1347 in NE Iberian Peninsula. Quaternary Science Reviews 93, 77–90. doi:10.1016/j.quascirev.2014.03.020

Corella, J.P., Stefanova, V., El Anjoumi, A., Rico, E., Giralt, S., Moreno, A., et al., 2013. A 2500-year multi-proxy reconstruction of climate change and human activities in northern Spain: The Lake Arreo record. Palaeogeography, Palaeoclimatology, Palaeoecology 386, 555–568. doi:10.1016/j.palaeo.2013.06.022

Corella, J.P., Brauer, A., Mangili, C., Rull, V., Vegas-Vilarrúbia, T., Morellón, M., et al., 2012. The 1.5-ka varved record of Lake Montcortès (southern Pyrenees, NE Spain). Quaternary Research 78, 323–332. doi:10.1016/j.yqres.2012.06.002

Corella, J.P., Amrani, A.E., Sigró, J., Morellón, M., Rico, E., Valero-Garcés, B.L., 2011. Recent evolution of Lake Arreo, northern Spain: influences of land use change and climate. Journal of Paleolimnology 46, 469–485. doi:10.1007/s10933-010-9492-7

Dearing, J.A., Jones, R.T., 2003. Coupling temporal and spatial dimensions of global sediment flux through lake and marine sediment records. Global and Planetary Change 39, 147–168. doi:10.1016/S0921-8181(03)00022-5

Esteban Cava, L., 1994. La Serranía Alta de Cuenca: Evolución de los usos del suelo y problemática socioterritorial, 1st ed. Artes Gráficas Antona S.A., Tarancón (Cuenca).

García-Ruiz, J.M., 2010. The effects of land uses on soil erosion in Spain: A review. CATENA 81, 1–11. doi:10.1016/j.catena.2010.01.001

García-Ruiz, J.M., López-Moreno, J.I., Vicente-Serrano, S.M., Lasanta–Martínez, T., Beguería, S., 2011. Mediterranean water resources in a global change scenario. Earth-Science Reviews 105, 121–139. doi:10.1016/j.earscirev.2011.01.006

García-Ruiz, J.M., Nadal-Romero, E., Lana-Renault, N., Beguería, S., 2013. Erosion in Mediterranean landscapes: Changes and future challenges. Geomorphology 198, 20–36. doi:10.1016/j.geomorph.2013.05.023

Goh, K.M., 1991. Carbon Dating, in: Carbon Isotope Techniques. ACADEMIC PRESS, INC, San Diego, California, pp. 126–146.

Julià, R., Burjachs, F., Dasi, M., Mezquita, F., Miracle, M., Roca, J., et al., 1998. Meromixis origin and recent trophic evolution in the Spanish mountain lake La Cruz. Aquatic Sciences 60, 279–299.

Kylander, M.E., Ampel, L., Wohlfarth, B., Veres, D., 2011. High-resolution X-ray fluorescence core scanning analysis of Les Echets (France) sedimentary sequence: new insights from chemical proxies. J. Quaternary Sci. 26, 109–117. doi:10.1002/jqs.1438

Lê, S., Josse, J., Husson, F., others, 2008. FactoMineR: an R package for multivariate analysis. Journal of statistical software 25, 1–18.

Lionello, P. (Ed.), 2012. The climate of the Mediterranean region: from the past to the future, 1st ed. ed, Elsevier insights. Elsevier, London ; Waltham, MA. 502 p.

López-Blanco, C., Gaillard, M.-J., Miracle, M.R., Vicente, E., 2011a. Lake-level changes and fire history at Lagunillo del Tejo (Spain) during the last millennium: Climate or humans? The Holocene 22 (5), 551–560. doi:10.1177/0959683611427337

López-Blanco, C., Miracle, M.R., Vicente, E., 2011b. Cladoceran assemblages in a karstic lake as indicators of hydrological alterations. Hydrobiologia 676, 249–261. doi:10.1007/s10750-011-0876-0

López-Moreno, J.I., Beguería, S., Vicente-Serrano, S.M., García-Ruiz, J.M., 2007. Influence of the North Atlantic Oscillation on water resources in central Iberia: Precipitation, streamflow anomalies, and reservoir management strategies: Influence of the NAO on water resources. Water Resources Research 43, n/a–n/a. doi:10.1029/2007WR005864

Lorenzo-Lacruz, J., Vicente-Serrano, S.M., López-Moreno, J.I., Beguería, S., García-Ruiz, J.M., Cuadrat, J.M., 2010. The impact of droughts and water management on various hydrological systems in the headwaters of the Tagus River (central Spain). Journal of Hydrology 386, 13–26. doi:10.1016/j.jhydrol.2010.01.001

Magny, M., Combourieu Nebout, N., de Beaulieu, J.L., Bout-Roumazeilles, V., Colombaroli, D., Desprat, S., et al., 2013. North–south palaeohydrological contrasts in the central Mediterranean during the Holocene: tentative synthesis and working hypotheses. Climate of the Past Discussions 9, 1901–1967. doi:10.5194/cpd-9-1901-2013

Mann, M.E., Zhang, Z., Rutherford, S., Bradley, R.S., Hughes, M.K., Shindell, D., Ammann, C., Faluvegi, G., Ni, F., 2009. Global Signatures and Dynamical Origins of the Little Ice Age and Medieval Climate Anomaly. Science 326, 1256–1260. doi:10.1126/science.1177303

Martín-Puertas, C., Valero-Garces, B.L., Pilar Mata, M., Gonzalez-Samperiz, P., Bao, R., Moreno, A., Stefanova, V., 2008. Arid and humid phases in southern Spain during the last 4000 years: the Zonar Lake record, Cordoba. The Holocene 18, 907–921. doi:10.1177/0959683608093533

Meyers, P., Lallier-Vergés, E., 1999. Lacustrine Sedimentary Organic Matter Records of Late Quaternary Paleoclimates. Journal of Paleolimnology 21, 345–372.

Miracle, M.R., Vicente, E., Pedrós-Alió, C., 1992. Biological studies of Spanish meromictic and stratified karstic lakes. Limnetica 8, 59–77.

Montserrat Martí, J.M., 1992. Evolución glaciar y postglaciar del clima y la vegetación en la vertiente sur del Pirineo: estudio palinológico, Monografías del Instituto Pirenaico de Ecología. Zaragoza.

Morellón, M., Anselmetti, F.S., Valero-Garcés, B., Giralt, S., Ariztegui, D., Sáez, A., et al., 2014. The influence of subaquatic springs in lacustrine sedimentation: Origin and paleoenvironmental significance of homogenites in karstic Lake Banyoles (NE Spain). Sedimentary Geology 311, 96–111. doi:10.1016/j.sedgeo.2014.07.004

Morellón, M., Pérez-Sanz, A., Corella, J.P., Büntgen, U., Catalán, J., González-Sampériz, P., et al., 2012. A multi-proxy perspective on millennium-long climate variability in the Southern Pyrenees. Climate of the Past 8, 683–700. doi:10.5194/cp-8-683-2012

Moreno, A., Pérez, A., Frigola, J., Nieto-Moreno, V., Rodrigo-Gámiz, M., Martrat, B., et al., 2012. The Medieval Climate Anomaly in the Iberian Peninsula reconstructed from marine and lake records. Quaternary Science Reviews 43, 16–32. doi:10.1016/j.quascirev.2012.04.007

Moreno, A., Valero-Garcés, B.L., González-Sampériz, P., Rico, M., 2008. Flood response to rainfall variability during the last 2000 years inferred from the Taravilla Lake record (Central Iberian Range, Spain). J Paleolimnol 40, 943–961. doi:10.1007/s10933-008-9209-3

Pascua Echegaray, E., 2012. Señores del Paisaje. Ganadería y recursos naturales en Aragón, siglos XIII al XVII. Universidad de Valencia, Valencia.

Peinado-Lorca, M., Martínez-Parra, J.M., 1987. La vegetación de España. Universidad de Alcalá de Henares, Madrid.

Pèlachs, A., Pérez-Obiol, R., Ninyerola, M., Nadal, J., 2009. Landscape dynamics of Abies and Fagus in the southern Pyrenees during the last 2200 years as a result of anthropogenic impacts. Review of Palaeobotany and Palynology 156, 337–349. doi:10.1016/j.revpalbo.2009.04.005

Pompeani, D.P., Abbott, M.B., Steinman, B.A., Bain, D.J., 2013. Lake Sediments Record Prehistoric Lead Pollution Related to Early Copper Production in North America. Environmental Science & Technology 47, 5545–5552. doi:10.1021/es304499c

R Development Core Team, 2015. R: A language and environment for statistical computing. R Foundation for Statistical Computing, Vienna.

Reimer, P.J., Bard, E., Bayliss, A., Beck, J.W., Blackwell, P.G., Ramsey, C.B., et al., 2013. IntCal13 and Marine13 radiocarbon age calibration curves 0–50,000 years cal BP. Radiocarbon 55, 1869–1887.

Roberts, N., Moreno, A., Valero-Garcés, B.L., Corella, J.P., Jones, M., Allcock, S., et al., 2012. Palaeolimnological evidence for an east–west climate see-saw in the Mediterranean since AD 900. Global and Planetary Change 84-85, 23–34. doi:10.1016/j.gloplacha.2011.11.002

Roberts, N., Stevenson, T., Davis, B., Cheddadi, R., Brewster, S., Rosen, A., 2004. Holocene climate, environment and cultural change in the circum-Mediterranean region, in: Battarbee, R.W., Gasse, F., Stickley, C.E. (Eds.), Past Climate Variability through Europe and Africa, Developments in Paleoenvironmental Research. Springer Netherlands, pp. 343–362.

Romero-Viana, L., Julià, R., Camacho, A., Vicente, E., Miracle, M.R., 2008. Climate Signal in Varve Thickness: Lake La Cruz (Spain), a Case Study. J Paleolimnol 40, 703–714. doi:10.1007/s10933-008-9194-6

Schnurrenberger, D., Russell, J., Kelts, K., 2003. Classification of lacustrine sediments based on sedimentary components. Journal of Paleolimnology 29, 141–154.

Shepard, F.P., 1954. Nomenclature Based on Sand-silt-clay Ratios. Journal of Sedimentary Research 24, 151–158.

Stern, N., 2006. The Stern review on the economics of climate change. Cambridge University Press, [Cambridge, UK].

Van der Post, K.D., Oldfield, F., Haworth, E.Y., Crooks, P.R.J., Appleby, P.G., 1997. A record of accelerated erosion in the recent sediments of Blelham Tarn in the English Lake District. Journal of Paleolimnology 18, 103–120.

Valbuena-Carabaña, M., de Heredia, U.L., Fuentes-Utrilla, P., González-Doncel, I., Gil, L., 2010. Historical and recent changes in the Spanish forests: A socio-economic process. Review of Palaeobotany and Palynology 162, 492–506. doi:10.1016/j.revpalbo.2009.11.003

Valero-Garcés, B.L., Moreno, A., 2011. Iberian lacustrine sediment records: responses to past and recent global changes in the Mediterranean region. Journal of Paleolimnology 46, 319–325. doi:10.1007/s10933-011-9559-0

Valero-Garcés, B., Morellón, M., Moreno, A., Corella, J.P., Martín-Puertas, C., Barreiro, F., et al., 2014. Lacustrine carbonates of Iberian Karst Lakes: Sources, processes and depositional environments. Sedimentary Geology 299, 1–29. doi:10.1016/j.sedgeo.2013.10.007

Vicente, E., Camacho, A., Rodrigo, M.A., 1993. Morphometry and physicochemistry of the crenogenic merornictic Lake “ElTobar” (Spain). Verh Int Verein Limnol 698–704.

Vicente, E., Miracle, M.R., 1988. Physicochemical and microbial stratification in a meromictic karstic lake of Spain. Verh Internat Verein Limnol 23, 522–529.